Article

Not peer-reviewed version

Seasonal Dynamics and Three-Dimensional Hydrographic Features of the Eastern Gulf of Thailand: Insights from High-Resolution Modeling and Field Measurements

Tanuspong Pokavanich *, Vasawan Worrawatanathum , Kittipong Phattananuruch , Sontaya Koolkalya

Posted Date: 17 May 2024

doi: 10.20944/preprints202405.1135.v1

Keywords: Direct rainfall; Gulf of Thailand; Chanthaburi Coastal Current; Monsoon; Three-dimensional modeling; Salinity dynamics; seasonal variability

Article

Seasonal Dynamics and Three-Dimensional Hydrographic Features of the Eastern Gulf of Thailand: Insights from High-Resolution Modeling and Field Measurements

Tanuspong Pokavanich [1,*], Vasawan Worrawatanathum [1], Kittipong Phattananuruch [2] and Sontaya Koolkalya [3]

[1] Department of Marine Science, Faculty of Fisheries, Kasetsart University
[2] Faculty of Fisheries, Kasetsart University
[3] Faculty of Agriculture Technology, Rambhai Barni Rajabhat University
* Correspondence: ffistop@ku.ac.th

Abstract: Through the integration of high-resolution hydrodynamic modeling and comprehensive field measurements, this study elucidates the intricate three-dimensional hydrographic characteristics of the eastern Gulf of Thailand (eGOT). In addition to the prevalent tidal currents dictating alternating flow along the northwestern and southeastern axes, our investigation reveals pronounced seasonal variations in mean currents, water temperature, and salinity within the eGOT, closely linked to the dynamics of the Asian-Australian monsoon system. During the southwest monsoon, mean currents exhibit a southeasterly trend, contrasting with a northwesterly pattern during the northeast monsoon. Lowest water temperatures occur during the latter, while the highest levels are observed during the 1st monsoon transition (April-March). Notably, salinity levels reach their lowest levels during the southwest monsoon and the 2nd monsoon transition (October), coinciding with the seasonal stratification of the water column and the emergence of a distinct stable along-the-shore northwesterly current with the average speed of 15 cm/s, defined here as the "Chathaburi Coastal Current (CCC)". Model experiments attribute the formation of the CCC to decreased salinity induced by direct rainfall, highlighting the significance of rainfall as a key factor influencing coastal water dynamics in tropical regions or areas experiencing high precipitation.

Keywords: direct rainfall; gulf of thailand; chanthaburi coastal current; monsoon; three-dimensional modeling; salinity dynamics; seasonal variability

---

1. Introduction

The eastern Gulf of Thailand (eGOT), depicted in Figure 1, spans over 25,000 km^2 and constitutes a shallow coastal water body situated at the northeastern extremity of the Gulf of Thailand. With an average depth of 35 m and the deepest area located offshore in the southwestern direction, reaching a maximum depth of 65 m, the eGOT encompasses approximately 500 km of coastline, which represents about 15% of Thailand's total coastline. It serves as a crucial site for marine environmental and socio-economic services in Thailand. The sea within the eGOT borders the coastal zones of Rayong, Chanthaburi, and Trat provinces in Thailand, as well as western regions of Cambodia, hosting vital industries, tourism facilities, cities, fisheries, and farmland. Despite its significant footprint, there exists limited documentation regarding its hydrographic characteristics. A comprehensive understanding of the hydrographic properties and their variations is essential for facilitating improved sea and resource management in this region.

Previous hydrographic investigations pertaining to the eastern Gulf of Thailand (eGOT) have predominantly focused on the broader characteristics of the Gulf of Thailand on a regional scale, with the eGOT area being merely a subset of their scope. Notably, [1] utilized data from the NAGA expedition to provide an initial description of the intricate hydrographic dynamics within the South China Sea and the Gulf of Thailand, highlighting their seasonal variability linked to the Asian-

Australian monsoon. Subsequent numerical studies, including those by [2], [3], [4], [5] have further elucidated the seasonal variations in Gulf of Thailand circulation. These variations are shown to be influenced by a combination of factors, including tides, prevailing winds, river discharge, direct rainfall to the sea, and sea surface heat exchanges. [6] conducted an analysis utilizing data obtained from High Frequency Radar, unveiling seasonal variations in tidal residual surface current patterns. Additionally, [7] corroborated these observations, providing further insight into the intricate complexities of these variations through the utilization of remotely sensed data.

Early works that providing detailed insights into the eGOT are scarce. [8] Utilized remotely sensed observations to discern the presence of a warm water pool during winter in the northeastern region of the Gulf of Thailand, adjacent to the eGOT. This phenomenon was attributed to orographic effects from the Cardamom Mountains in Cambodia. Furthermore, [9] conducted limited field measurements using current meters at Ban Leam Sork in Trat province, revealing robust tidal currents with maximum speeds reaching 24 cm/s. They observed alternating flow directions during flood and ebb tides, along with residual currents predominantly towards the southeastern direction in December. Additionally, [9] documented the intricate seasonal patterns of residual currents around Koh Monnai Island in Rayong province. These patterns were found to be influenced by monsoonal winds, which were further modified by tides and local topography.

Expanding upon previous research, field evidence and unpublished reports have revealed peculiar hydrographic features within the eastern Gulf of Thailand (eGOT). Notably, despite the absence of significant river inflows, instances of low salinity seawater (<28 ppt) have been documented, with notable salinity disparities (>2-3 ppt) between near-surface and sub-surface layers. We hypothesize that this reduced salinity stems from direct rainfall into the sea. Although lacking major river inputs, the eGOT experiences rainfall rates exceeding the national average. Direct rainfall likely diminishes coastal water salinity, thereby reducing overall water density. Consequently, a freshwater layer can form atop denser seawater, resulting in stratification that hampers vertical mixing and restricts exchanges of heat, nutrients, and dissolved gases between surface and deeper layers. Such stratification may induce buoyancy-driven flows and horizontal currents, influencing coastal hydrodynamics and distinguishing the eGOT from the broader Gulf of Thailand (GOT) system. Similar phenomena of rainfall influence on coastal dynamics have been documented both in the open ocean [10,11] and coastal environments [12–14]. Moreover, studies by [5,15] have demonstrated the substantial impact of atmospheric freshwater fluxes of the Asian-Australian monsoon system on the Bay of Bengal and the Gulf of Thailand, respectively. Alterations in coastal hydrodynamics induced by direct rainfall can yield ecological ramifications. Changes in circulation patterns and stratification can affect nutrient availability, primary production, and the distribution of plankton and other marine organisms, thereby influencing ecosystem dynamics [16–18]

This paper aims to offer detailed insights into the topographic, meteorological and three-dimensional hydrographic characteristics of the eGOT intricate three-dimensional hydrography of the region. Furthermore, we present influence of direct rainfall on local three-dimensional hydrography at the eGOT and the emergence of the Chathaburi Coastal Current (CCC) through numerical experiments. This finding holds relevance for hydrodynamic modeling endeavors in tropical shallow coastal regions that receive significant freshwater inputs, not only from river systems but also from direct rainfall.

Preprints.org (www.preprints.org) | NOT PEER-REVIEWED | Posted: 17 May 2024 doi:10.20944/preprints202405.1135.v1

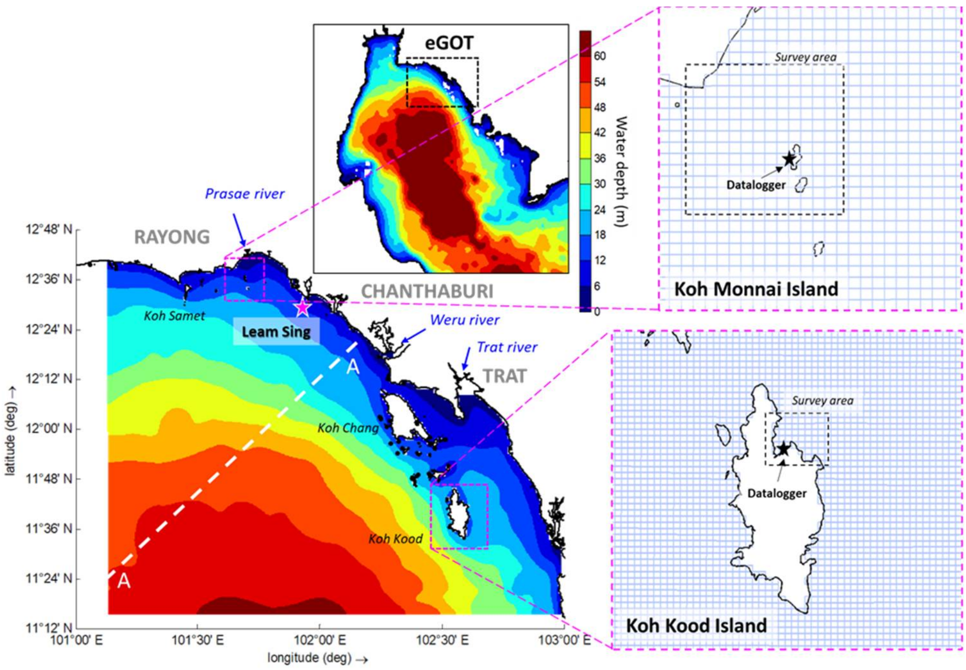

Figure 1. Location map, bathymetry, and modeling domain of the Eastern Gulf of Thailand (eGOT) within the larger Gulf of Thailand. Star symbols indicate the locations of field-observed data, while inset plots provide detailed views of the modeling grid and survey areas near Koh Monnai Island and Koh Kood Island.

2. Materials and Methods

2.1 Study Site

The eastern Gulf of Thailand (eGOT) comprises a vast coastal expanse spanning Rayong, Chanthaburi, and Trat provinces. Similar in depth to the broader Gulf of Thailand (GOT), the eGOT features average depths of 25 meter, with a maximum depth of 65 meters offshore. The area is dotted with numerous islands, exceeding 50 in total, with notable examples including Koh Samet, Koh Chang, and Koh Kood islands (see Figure 1). Contributing to the hydrology of the eGOT are two medium-sized rivers: the Prasae River, the Weru River, and the Trat River. Over a 15-year period from 2006 to 2020, averaged modeled discharge data from the Global Flood Awareness System [19] estimate an annual total discharge from rivers in the eGOT of approximately 7.58 km^3. This discharge represents approximately 13% of the annual average discharge from major rivers draining into the broader Gulf of Thailand, which is estimated at approximately 57.98 km^3.

Wind and rainfall data from the ECMWF-ERA5 reanalysis dataset [20,21] exhibit strong agreement with measurements from Thailand's Meteorological Agency stations. Averaged over 15 years, the ECMWF-ERA5 data, as depicted in Figure 2, illustrates the significant influence of the Asian-Australian monsoon system, characterized by two monsoon seasons and two transitional periods. Specifically, the northeast monsoon (NEM) occurs from November to February, the first monsoon transition (Transition 1) from March to April, the southwest monsoon (SWM) from May to September, and the second monsoon transition (Transition 2) in October. To represent these distinct climatic conditions, December, April, August, and October were selected to respectively signify the NEM, Transition 1, SWM, and Transition 2.

During the SWM and Transition 2, the total rainfall amounts to 85% of the annual precipitation in the eGOT, totaling 49.5 km^3. Notably, when considering the freshwater sources to the eGOT, it is found that direct rainfall into the sea contributes significantly more (58.0 km^3) than river discharge (7.6 km^3), by a factor of 7.5. Figure 3 illustrates the detailed seasonal variation of freshwater fluxes to the eGOT. Wind patterns closely align with monsoon dynamics, with stronger winds (8-10 m/s) prevailing during monsoon seasons and following the respective monsoon directions. Winds during Transition 2 are relatively calm compared to other periods of the year.

Preprints.org (www.preprints.org) | NOT PEER-REVIEWED | Posted: 17 May 2024 doi:10.20944/preprints202405.1135.v1

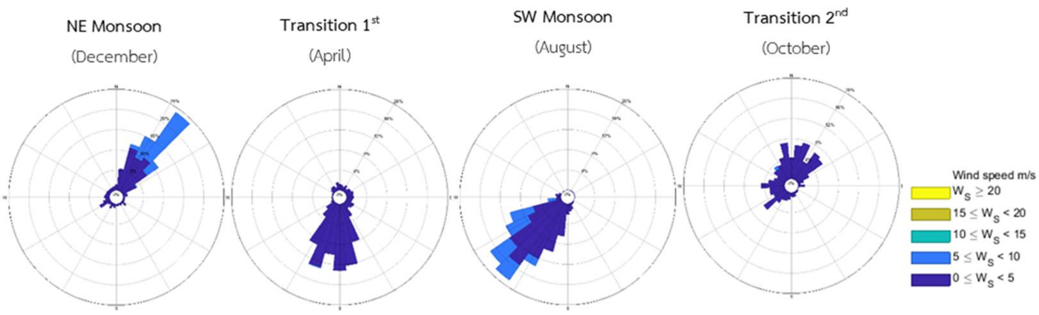

Figure 2. Monthly average wind rose derived from the ECMWF-ERA5 dataset between 2006-2020 showing at different monsoonal periods from Koh Monnai island.

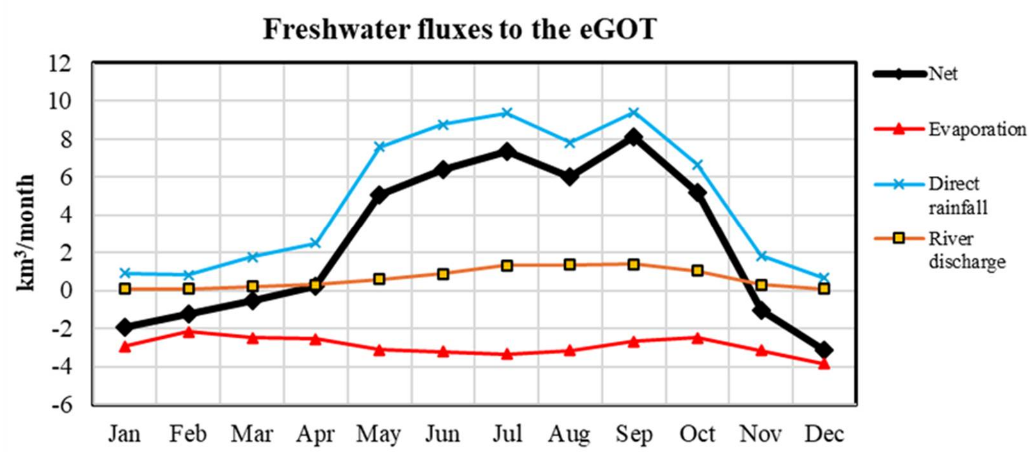

Figure 3. Freshwater fluxes to the eGOT. Data are from ECMWF-ERA5 reanalysis dataset averaged monthly between 2006-2020.

2.2. Field Observation

Seasonal synoptic measurements were conducted around Koh Monnai Island and Koh Kood Island to gather water temperature and salinity data using a multi-parameter water quality profiling sonde (AAQ-RINKO, JFE Advantech-Japan). Additionally, current flow velocity profiles were obtained using an acoustic Doppler current profiler (ADCP) with bottom tracking functionality (Sentinel Workhorse 1200 kHz, Teledyne RD Instrument-U.S.A.), measuring downward-facing currents. Salinity distribution at various depths around Koh Monnai Island and Koh Kood Island is presented in Figure 4 and Figure 5, respectively. ADCP measurement results at Koh Kood Island are depicted in Figure 6, with the survey area location map provided in Figure 1.

In addition to the seasonal synoptic survey, long-term deployment of dataloggers was undertaken to monitor temporal variations of water level, water temperature, and salinity at Koh Monnai Island (101°41'10.26"E, 12°36'48.65"N) and Koh Kood Island (102°34'13.04"E, 11°42'20.76"N). Water depths around Koh Monnai Island ranges between 4 and 10 meters. HOBO-Water level loggers (Onset, U.S.A.) and HOBO-Conductivity loggers (Onset, U.S.A.) were deployed within perforated PVC pipes at 30-minute intervals. Continuous deployment of dataloggers at Koh Monnai Island spanned from October 2019 to November 2021, while deployment at Koh Kood Island lasted for a minimum of 15 days during different monsoon seasons between 2021 and 2022. Local maintenance efforts ensured the quality of observed data by regularly cleaning the loggers. Furthermore, additional water level measurements from the Thailand Hydrographic Department at Leamsing station (101°57'40.89"E, 12°27'48.31"N) were utilized for model validation purposes.

Preprints.org (www.preprints.org) | NOT PEER-REVIEWED | Posted: 17 May 2024 doi:10.20944/preprints202405.1135.v1

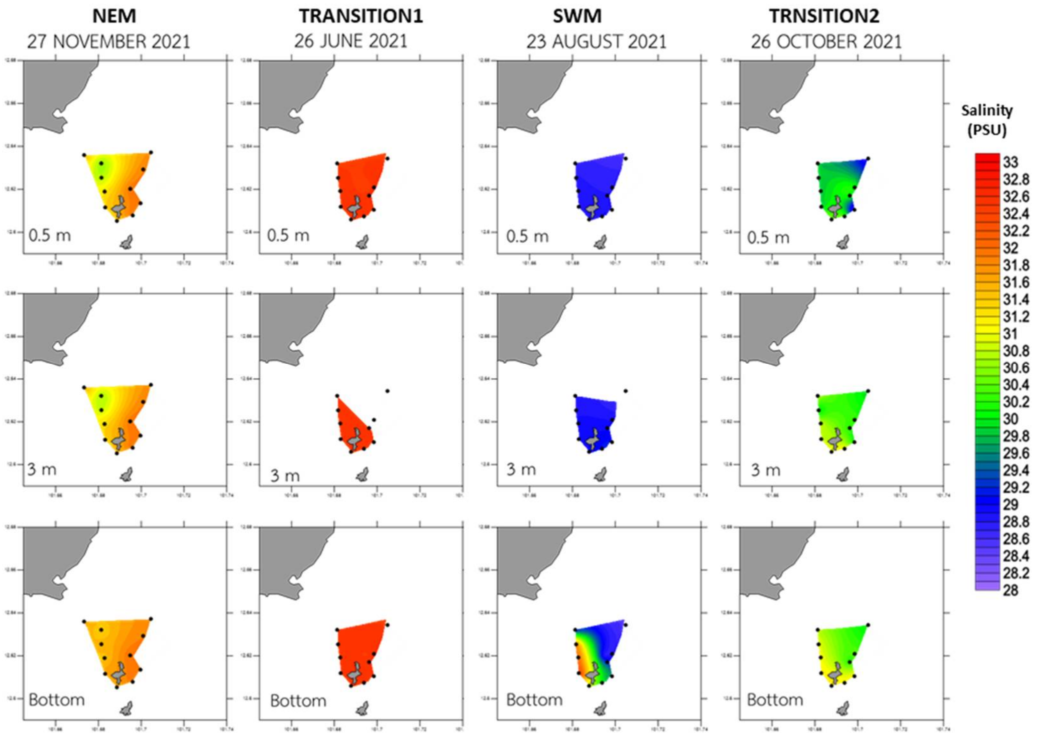

Figure 4. The salinity distribution at various times and depths around Koh Monnai Island was derived from synoptic survey data interpolation. The locations of the measurements are denoted by black dots.

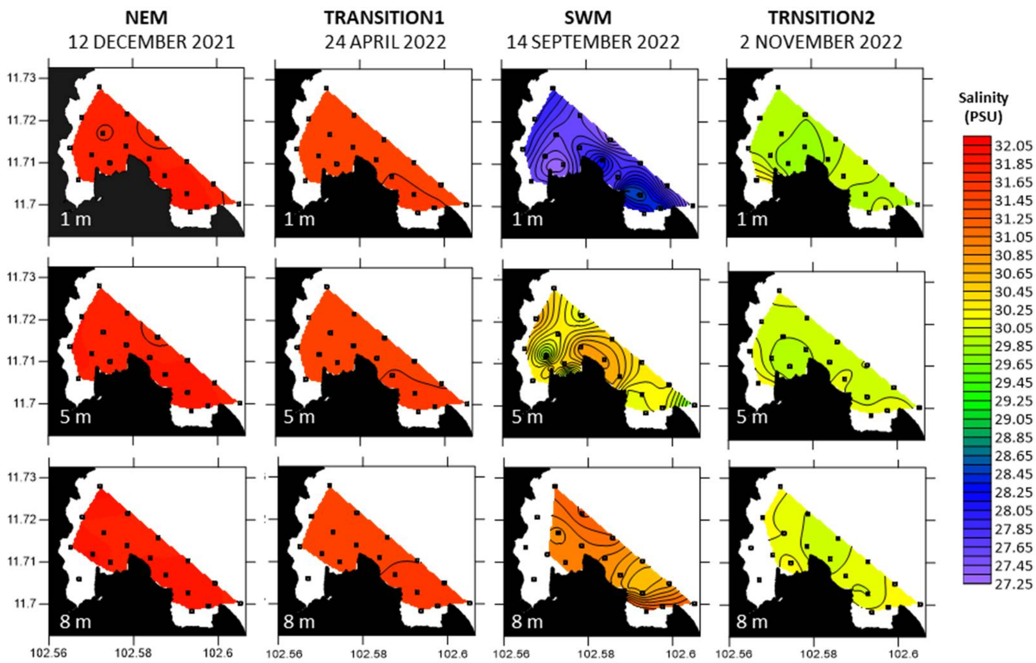

Figure 5. The salinity distribution at various times and depths around Koh Kood Island was derived from synoptic survey data interpolation. The locations of the measurements are denoted by black dots.

Preprints.org (www.preprints.org) | NOT PEER-REVIEWED | Posted: 17 May 2024 doi:10.20944/preprints202405.1135.v1

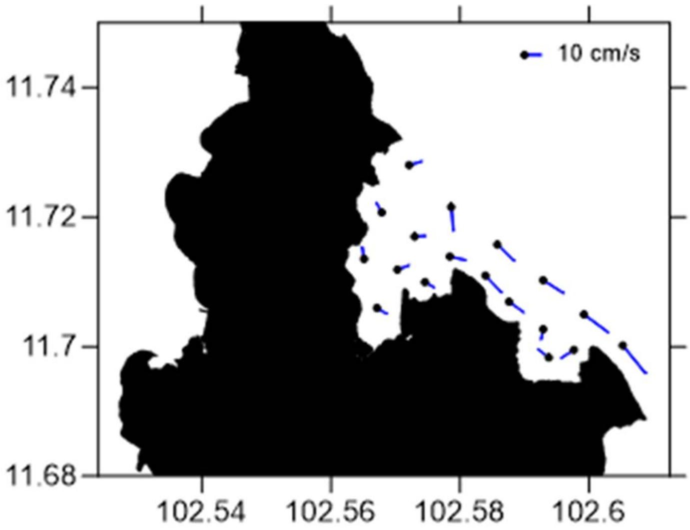

Figure 6. Near-surface flow velocity field from ADCP measurement facing down with bottom tracking functionality at Koh Kood island during ebb tide on 14 September 2022.

3. Results and Discussion

3.1 Hydrodynamic Modeling

A three-dimensional hydrodynamic model was established using the Delft3D-FLOW program [22]. The model employs a rectangular grid in spherical coordinates, covering the entirety of the eGOT. It consists of 273x326 horizontal grid cells and incorporates 10 vertical layers in sigma coordinate. The thickness of each layer, from surface to bottom, constitutes 2%, 6%, 8%, 10%, 10%, 10%, 10%, 12%, 14%, and 18% of the total water depth, respectively. Simulations encompass a period of one year, from January 1, 2020, to December 31, 2020, capturing all monsoonal fluctuations. The model includes a spin-up time of one year, where the final conditions of the cool start year initiate the warm start of the run. External forcings comprise offshore water level data from the OSU TPXO tide model [23] and layer-varying water temperature and salinity derived from an in-house three-dimensional model of the Gulf of Thailand. Bed shear stress is calculated using a quadratic bed stress formula, with a Chezy bottom roughness number set at 70 m½/s and constant horizontal eddy viscosity at 10 m^2/s. Meteorological data are sourced from ECMWF-ERA5 reanalysis data at 3-hour intervals [20,21]. The wind drag coefficient follows a quadratic formula [24], with coefficients of 0 and 0.004 at wind speeds of 0 m/s and 25 m/s, respectively. The model accounts for freshwater input solely from direct rainfall, as river discharge data contribution is deemed significantly lower in comparison.

Model validation against long-term measured data includes water level at Leamsing station, and water temperature and salinity at Koh Monnai Island. The model demonstrates good agreement with observed water level at Leamsing, with a Root Mean Square Error (RMSE) of < 14.8 cm from a tidal range during spring tide of approximately 250 cm and an R2 value of 0.91. For water temperature, the RMSE is 0.76°C with an R^2 value of 0.81 (see Figure 7). Salinity levels and trends are also well-reproduced by the model.

Preprints.org (www.preprints.org) | NOT PEER-REVIEWED | Posted: 17 May 2024 doi:10.20944/preprints202405.1135.v1

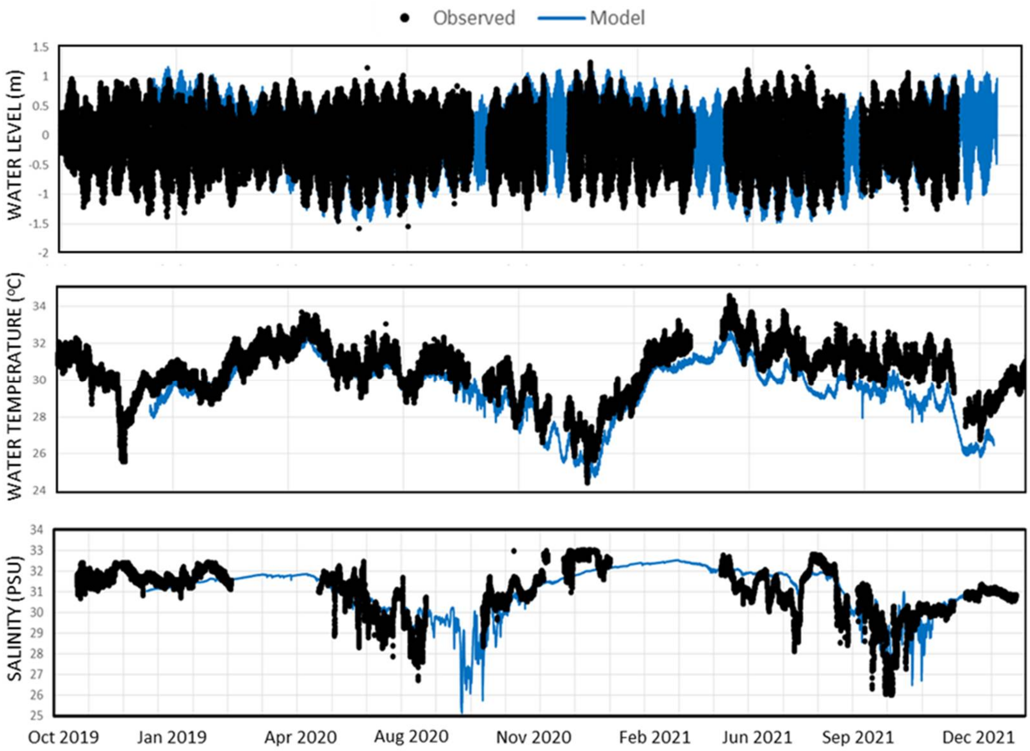

Figure 7. Comparison between continuous measurements of water level, water temperature, and salinity at Koh Monnai Island and the modeled results. The continuous measurement data is represented by blank dots, while the model results are indicated by a blue line.

3.2 Tide and Tidal Currents

Tidal currents play a pivotal role in mobilizing and mixing the entire water column within coastal seas. In the eGOT, tides drive water movement alternately along the coastline in a northwest to southeast axis. During the flood tide, tidal currents flow northwestward, while they shift southeastward during the ebb tide. Tidal currents ease during high and low tides. Maximum tidal current speeds during spring tides range between 0.3-0.5 m/s, halving during neap tides. Offshore tidal current speeds generally exceed those near the shoreline, except in channels between land-island and island-island (see Figure 8a). Local shoreline irregularities and bathymetry intricately influence tidal flow patterns. At the lee side of headlands, currents change direction, forming clockwise and counterclockwise eddies, evident in both field measurements (see Figure 5) and well-reproduced by modeling (see Figure 8b).

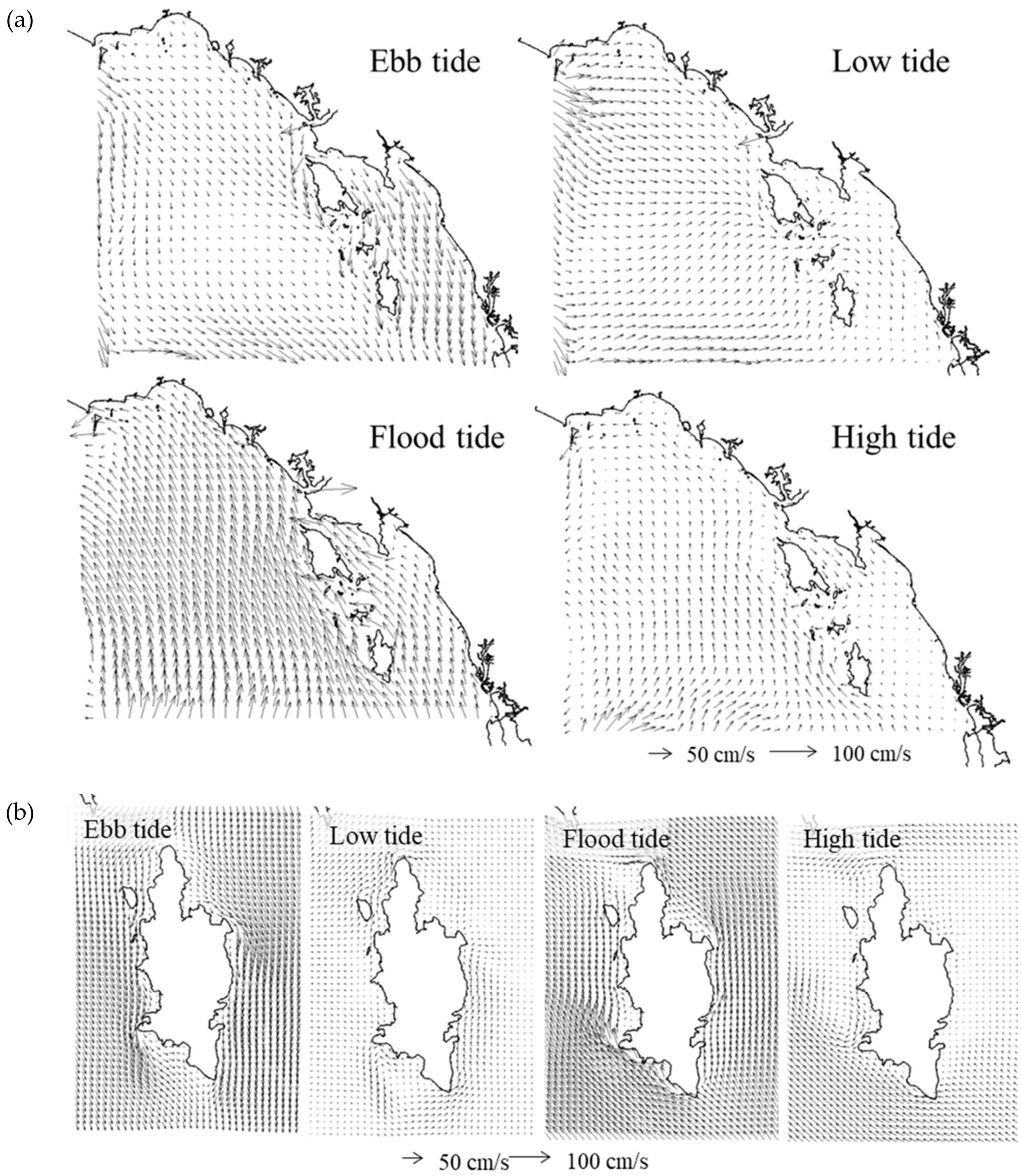

Figure 1. Tidal current patterns (a) at the eGOT and (b) around Koh Kood Island during spring tide.

3.3 Water Temperature and Salinity

The results from field observations (Figure 4, Figure 5, and Figure 7) and modeling (Figure 9 and Figure 10) demonstrate good agreement in depicting the spatial and seasonal variability of water temperature and salinity in the eGOT, with ranges spanning between 24-30°C and 29-32.5 ppt, respectively. Water temperature is lowest during the NEM, rapidly rising to its annual peak during Transition 1. This temperature fluctuation is most pronounced along the shoreline, where waters are coolest during the NEM and warmest during Transition 1. In contrast, salinity exhibits marked changes during the SWM and Transition 2, with reductions observed along the shoreline, particularly along the coasts of Chanthaburi and Trat provinces. It's important to note that since the model does not account for freshwater input from rivers, the observed reduction in salinity is attributed to direct rainfall into the sea surface.

The model results reveal notable water column stratification characterized by alternating water temperature and salinity profiles. This phenomenon persists throughout the year, except during the NEM when the water column exhibits relatively homogeneous conditions. During Transition 1, a

 doi:10.20944/preprints202405.1135.v1

distinct temperature stratification emerges, with the near-surface layer up to 30 meters depth exhibiting higher temperatures compared to the lower layers. Following Transition 1, water temperature becomes more evenly distributed throughout the water column. Conversely, salinity does not exhibit significant stratification during Transition 1 but becomes strongly stratified during the SWM and Transition 2. Both water temperature and salinity revert to a more uniform vertical distribution during the NEM.

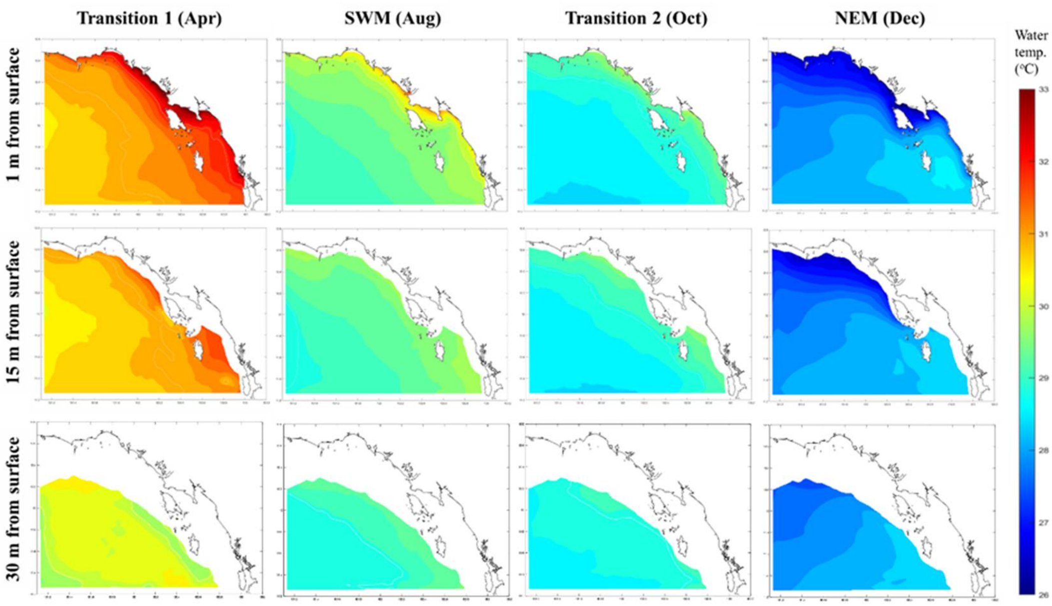

Figure 9. Modeled monthly averaged water temperature at 1 m, 10 m and 20 meter from the sea-surface at different monsoonal periods.

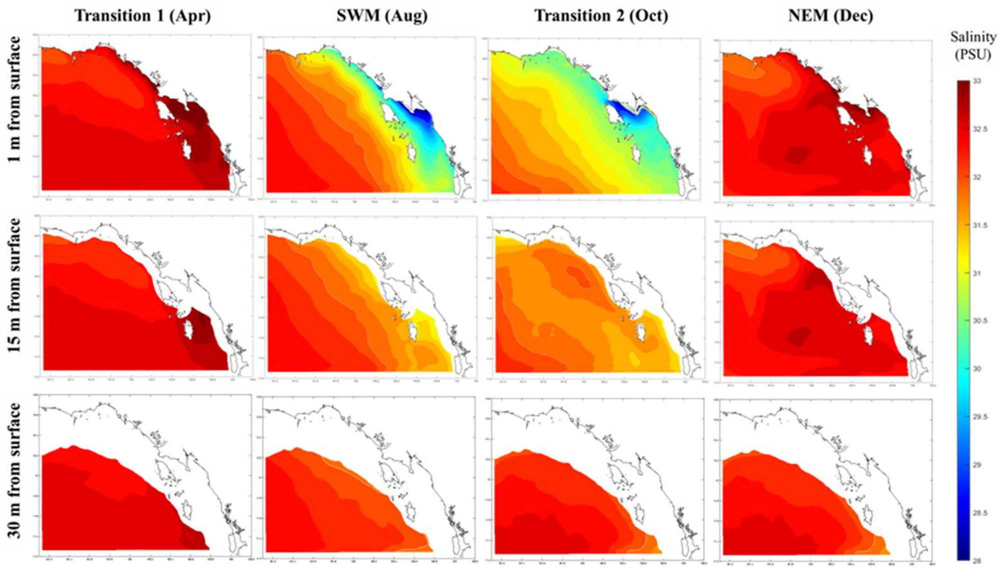

Figure 10. Modeled monthly averaged salinity at 1 m, 10 m and 20 meter from the sea-surface at different monsoonal periods.

3.4. Seasonal Water Circulation

The monthly mean simulated flow velocity fields depict the diverse circulation patterns of the eGOT influenced by monsoonal effects, as illustrated in Figure 11. Two primary circulation patterns emerge, characterized by flow directions to the southeast during Transition 1 and the SWM, and to

Preprints.org (www.preprints.org) | NOT PEER-REVIEWED | Posted: 17 May 2024 doi:10.20944/preprints202405.1135.v1

the northwest during Transition 2 and the NEM. Monthly average current speeds peak (>0.15 m/s) during the SWM and the NEM, with the strongest currents observed offshore during the SWM and approximately 40 km from the shoreline during the NEM. Current speeds diminish during the monsoon transitions, albeit with a notable exception during the SWM and Transition 2, where a robust coastal current (within 10 km from the shoreline) flows northeastward with speeds exceeding 15 cm/s. This coastal current, flowing along Chanthaburi Province in Thailand, is dubbed the "Chanthaburi Coastal Current (CCC)" and forms during the SWM, becoming particularly strong and stable during Transition 2.

Additionally, the model results highlight significant differences between near-surface and sub-surface circulation, which vary seasonally. Near-surface currents tend to flow towards the land during Transition 1 and the SWM, shifting to offshore flow during Transition 2 and the NEM. Sub-surface counter-currents persist during periods of water column stratification. In Figure11, averaged current profiles along and across section A-A, location shows in Figure1, further elucidate the layered flow patterns during stratified periods, displaying a three-layer and two-layer flow system during the SWM and Transition 2, respectively. Conversely, during the NEM, when the water column is well-mixed, flow tends to be more homogeneous.

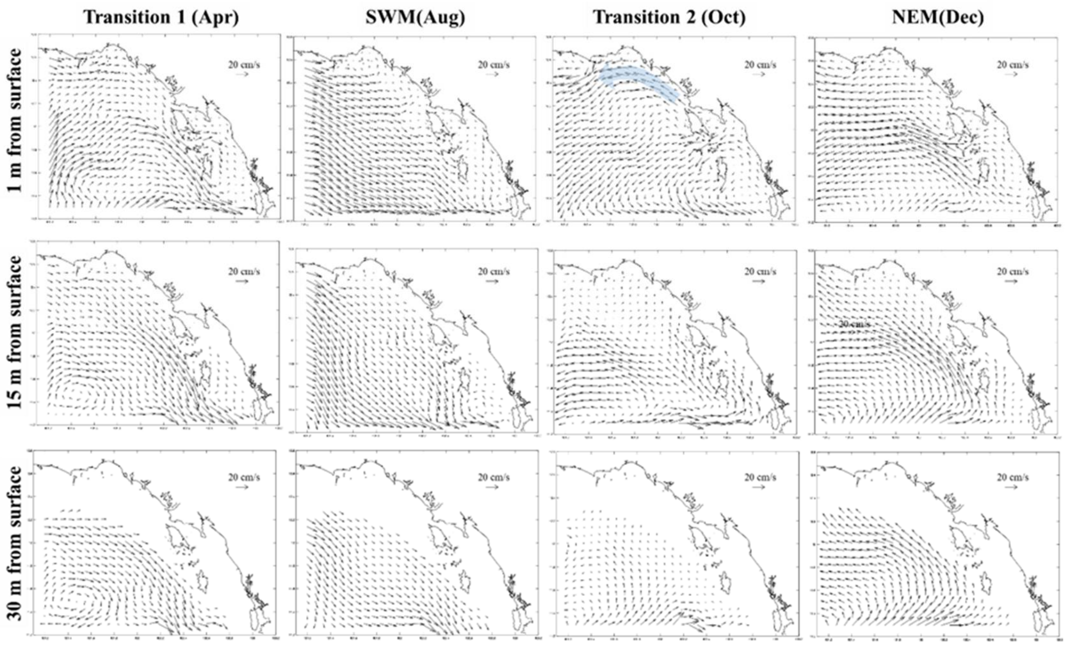

Figure 11. Modeled monthly averaged flow velocity field at 1 meter, 15 meter and 30 meter from the sea-surface at different monsoonal periods. Light blue translucent arrows present near-surface during the Transition 2 is the Chanthaburi Coastal Current.

3.5 Influence of the Direct Rainfall into the Sea

The substantial spatial and temporal variations observed in salinity patterns within the eGOT are expected to exert significant influence on water column dynamics and circulation regimes. Given the prominent role of rainfall in shaping salinity, this study endeavors to explore the impact of direct rainfall through the establishment of an additional model. Simulations conducted with and without direct precipitation yield insightful outcomes, as depicted in Figures 12 and 13, respectively.

A comparative analysis of these outcomes highlights the pronounced effect of direct rainfall, particularly during the SWM and Transition 2 phases, characterized by intensified rainfall and reduced wind activity within the eGOT. While the influence of rainfall on other temporal intervals and water temperature remains relatively subdued, the marked decrease in salinity significantly contributes to water column stratification during the SWM and Transition 2. This stratification profoundly alters overarching circulation patterns, precipitating the emergence of the CCC during these intervals. Notably, the removal of rainfall from the simulations results in the cessation of the CCC and the attendant two-layer circulation.

Preprints.org (www.preprints.org) | NOT PEER-REVIEWED | Posted: 17 May 2024 doi:10.20944/preprints202405.1135.v1

The influence of freshwater influx from direct rainfall into the marine environment has been previously documented to affect various phenomena, such as the sea surface microlayer [11] and the formation of freshwater lenses under calm wind conditions within the California Current [10]. These effects subsequently exert a notable impact on the hydrodynamic characteristics of the marine domain. Our study marks the first documentation of the effects of direct rainfall on the generation of upper-layer low salinity water, thereby contributing to the genesis of the CCC. Interestingly, a similar occurrence of upper-layer low salinity coastal currents was recently observed during Transition 2 along the western coast of the Gulf of Thailand [25]. However, in that instance, the diminished salinity levels were attributed to river discharge.

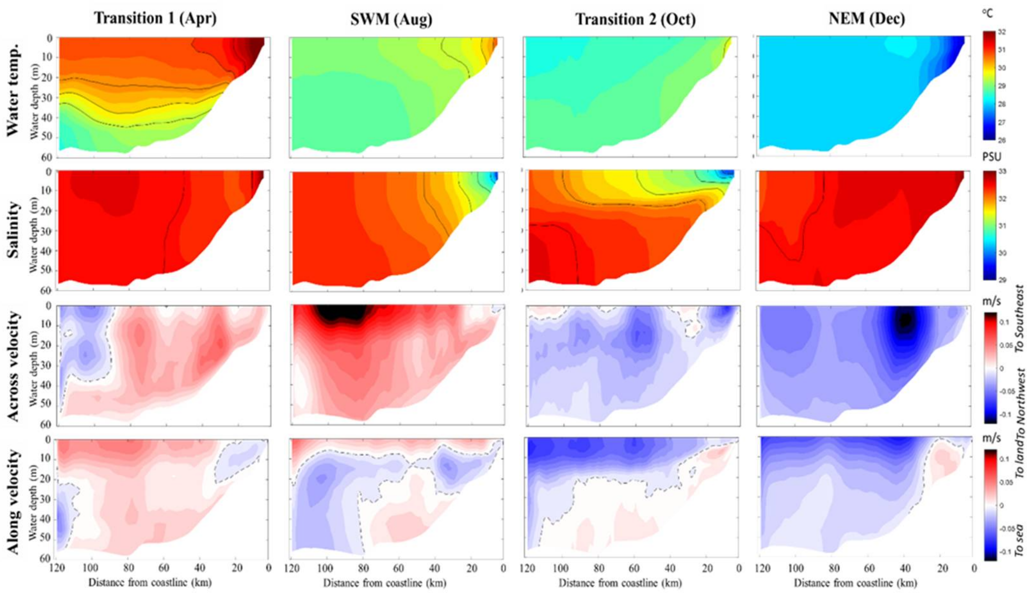

Figure 12. Distribution of the water temperature and salinity and mean flow velocities at the A-A section at different monsoonal periods from the model run with the direct rainfall into the sea.

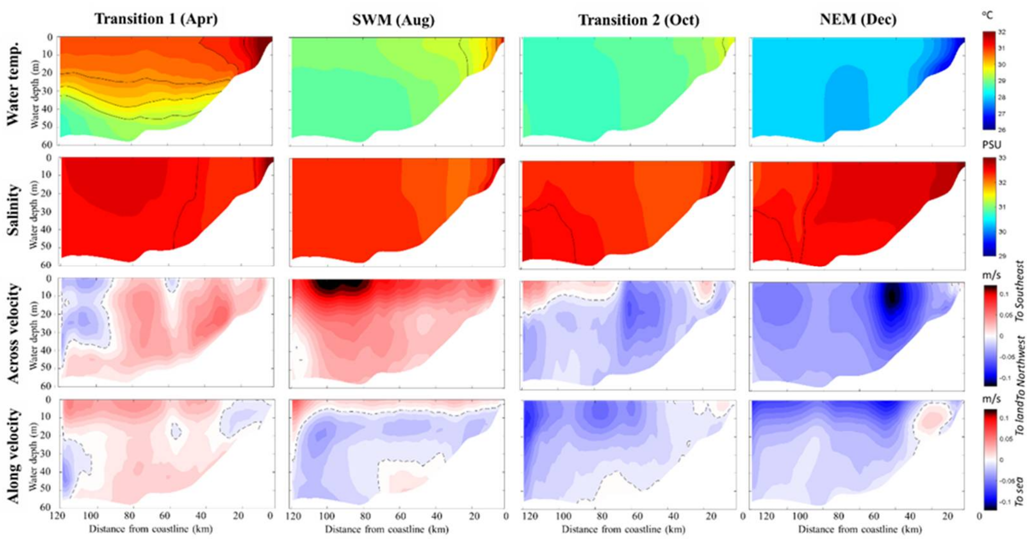

Figure 13. Distribution of the water temperature and salinity and mean flow velocities at the A-A section at different monsoonal periods from the model run without the direct rainfall into the sea.

5. Conclusions

Noted from field observations, hydrographic conditions at the eGOT exhibit significant spatial and temporal variability, with pronounced variations in water temperature, salinity, and flow velocities influenced by the Asian-Australian monsoon. Offshore and deep areas typically experience

Preprints.org (www.preprints.org) | NOT PEER-REVIEWED | Posted: 17 May 2024 doi:10.20944/preprints202405.1135.v1

lower water temperatures, reaching their lowest levels during the NEM. During Transition 1, lower layer temperatures are 2-3 degrees lower than near-surface values. The SWM brings higher freshwater input from rainfall, resulting in a significant reduction in salinity of near-surface layers. This salinity decrease is particularly prominent during the SWM and Transition 2. Differences between near-surface and sub-surface, and near-shore and offshore salinity can be 2-3 ppt, significantly impacting seawater density. The influx of freshwater from rainfall diminishes the overall salinity of coastal waters, leading to decreased water density. During the SWM and Transition 2, strong stratification is observed in shallow areas (water depth < 15 m), influencing coastal hydrodynamics. Salinity levels are low during these periods when rainfall rates significantly increase and wind is relatively calm. Stratification affects vertical mixing and circulation patterns of the water column, altering hydrodynamics. It can hinder vertical mixing and restrict exchange of heat, nutrients, and dissolved gases between surface and deeper layers [10–13,26].

The water circulation in the eGOT exhibits two distinct modes, flowing southeastward during the Transition 1 and SWM, and northwestward during Transition 2 and NEM, closely aligned with predominant wind directions. The strongest circulation occurs during the SWM and NEM periods. Layered flows induced by water column stratification are particularly notable during the SWM and Transition 2. During these periods, a northwesterly Chanthaburi Coastal Current (CCC) emerges. Model simulations suggest that the CCC can be sustained by direct rainfall into the sea during the SWM and Transition 2. The presence of the CCC may significantly influence the seasonal transport of sediments, nutrients, and pollutants along the eGOT coastline, with ecological ramifications. Altered circulation patterns and stratification affect nutrient availability, primary production, and the distribution of plankton and other marine organisms, ultimately impacting the entire ecosystem and fisheries dynamics [17,18].

Future work is essential to conduct detailed sensitivity analyses and model runs to investigate the mechanisms governing the Chanthaburi Coastal Current (CCC) and its variations. This may include considering freshwater discharges from small rivers and creeks along the eGOT coastline, as well as grid refinement and additional continuous field observations for model validation along the coastline. These efforts could enhance the model's capability to capture the detailed behavior of the CCC. Furthermore, investigation of the effects of changing rainfall patterns in the future, resulting from inter-annual variations in climate drivers such as the El Niño-Southern Oscillation and the Indian Ocean Dipole, is warranted. Additionally, exploring the influence of extreme rainfall events, which are expected to occur more frequently under ongoing global warming, is crucial [14,16,27]. Such future research endeavors will provide valuable insights into the dynamics of the eGOT's hydrographic features and their responses to environmental changes.

References

1. Wyrtki, K., Physical oceanography of the Southeast Asian waters. Vol. 2. 1961: University of California, Scripps Institution of Oceanography.
2. Yanagi, T., et al., Seasonal variation of stratification in the Gulf of Thailand. Journal of oceanography, 2001. 57: p. 461-470.
3. Aschariyaphotha, N., et al., Simulation of seasonal circulations and thermohaline variabilities in the Gulf of Thailand. Advances in atmospheric sciences, 2008. 25: p. 489-506.
4. Sojisuporn, P., A. Morimoto, and T. Yanagi, Seasonal variation of sea surface current in the Gulf of Thailand. Coastal Marine Science, 2010. 34(1): p. 91-102.
5. Buranapratheprat, A., et al., The modification of water column conditions in the Gulf of Thailand by the influences of the South China Sea and monsoonal winds. Continental Shelf Research, 2016. 118: p. 100-110.
6. Saramul, S., Seasonal monsoon variations in surface currents in the Gulf of Thailand revealed by high frequency radar. Engineering Journal, 2017. 21(4): p. 25-37.
7. Anutaliya, A., Surface circulation in the Gulf of Thailand from remotely sensed observations: seasonal and interannual timescales. Ocean Science, 2023. 19(2): p. 335-350.
8. Li, J., et al., Effects of Cardamom Mountains on the formation of the winter warm pool in the gulf of Thailand. Continental Shelf Research, 2014. 91: p. 211-219.
9. Buranapratheprat, A., et al., Water Circulation at Bangsaen Beach, Chonburi Province in 2014–2015. Burapha Science Journal, 2017: p. 38-48.
10. Hoffman, L., et al., Ocean Surface Salinity Response to Atmospheric River Precipitation in the California Current System. Journal of Physical Oceanography, 2022. 52(8): p. 1867-1885.

 doi:10.20944/preprints202405.1135.v1

11. Gassen, L., et al., The impact of rainfall on the sea surface salinity: a mesocosm study. Scientific Reports, 2024. 14(1): p. 6353.
12. Schmidt, N. and M.E. Luther, ENSO impacts on salinity in Tampa Bay, Florida. Estuaries, 2002. 25: p. 976-984.
13. Behara, A., P. Vinayachandran, and D. Shankar, Influence of rainfall over eastern Arabian Sea on its salinity. Journal of Geophysical Research: Oceans, 2019. 124(7): p. 5003-5020.
14. Liu, F., et al., Importance of precipitation on the upper ocean salinity response to typhoon kalmaegi (2014). Water, 2020. 12(2): p. 614.
15. Haditiar, Y., et al., The effect of monsoon on the bay of Bengal based on a hydrodynamic model. Journal of Engineering Science and Technology, 2022. 17(2): p. 0936-0955.
16. Paerl, H.W., et al., Ecological response to hurricane events in the Pamlico Sound system, North Carolina, and implications for assessment and management in a regime of increased frequency. Estuaries and Coasts, 2006. 29: p. 1033-1045.
17. Ballard, T.C., E. Sinha, and A.M. Michalak, Long-term changes in precipitation and temperature have already impacted nitrogen loading. Environmental science & technology, 2019. 53(9): p. 5080-5090.
18. Han, H., et al., Influence of a heavy rainfall event on nutrients and phytoplankton dynamics in a well-mixed semi-enclosed bay. Journal of hydrology, 2023. 617: p. 128932.
19. Harrigan, S., et al., River discharge and related historical data from the Global Flood Awareness System, v2. 1, Copernicus Climate Change Service (C3S) Climate Data Store (CDS). 2019.
20. Hersbach, H., et al., ERA5 hourly data on pressure levels from 1979 to present. Copernicus Climate Change Service (C3S) Climate Data Store (CDS).(Accessed on 20-MAY-2021). 2018.
21. Hersbach, H., et al., ERA5 hourly data on single levels from 1979 to present. Copernicus climate change service (c3s) climate data store (cds), 2018. 10(10.24381).
22. Hydraulics, W.L., User Manual of Delft3D-FLOW—Simulation of Multi-dimensional Hydrodynamic Flows and Transport Phenomena, Including Sediments. 2003. p. 497 pp.
23. Egbert, G.D. and S.Y. Erofeeva, Efficient inverse modeling of barotropic ocean tides. Journal of Atmospheric and Oceanic technology, 2002. 19(2): p. 183-204.
24. Smith, S.D. and E.G. Banke, Variation of the sea surface drag coefficient with wind speed. Quarterly Journal of the Royal Meteorological Society, 1975. 101: p. 665-673.
25. Pokavanich, T. and K. Phattananuruch, Seasonal hydrographic patterns of the Gulf of Thailand and interactions with the South China Sea: insights from a numerical Model utilizing the novel dataset. in the 2nd UN Ocean Decade Regional Conference and 11th IOC-WESTPAC Conference. 2024. Bangkok, Thailand.
26. Royer, T.C., On the effect of precipitation and runoff on coastal circulation in the Gulf of Alaska. Journal of Physical Oceanography, 1979. 9(3): p. 555-563.
27. Donat, M.G., et al., More extreme precipitation in the world's dry and wet regions. Nature Climate Change, 2016. 6(5): p. 508-513.